Synthesis of Spirooxindoles through Cyclocondensation of Isatin and Cyclic 1,3-Diones

Rahul Joshi,[a]* (iD) Anita Kumawat,[a] Saurabh Singh,[b] Tapta Kanchan Roy,[c,d] and Ram T. Pardasani[c]*

[a]Department of Chemistry, University of Rajasthan, Jaipur 302004, India
[b]M.L.V. Government P.G. College, Bhilwara, Rajasthan, India
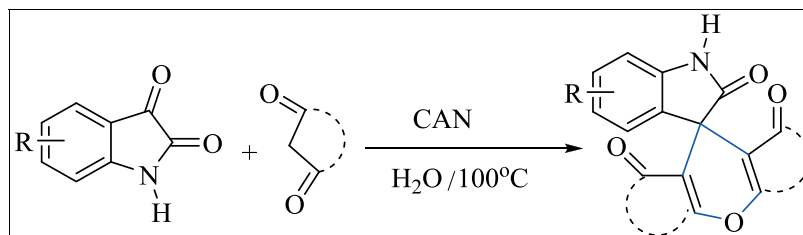[c]Department of Chemistry, Central University of Rajasthan, Bandar Sindri, Kishangarh, Ajmer, Rajasthan, India
[d]Department of Chemistry and Chemical Sciences, Central University of Jammu, Jammu 180011, India
*E-mail: rtpardasani@curaj.ac.in; rjsfs2018@gmail.com

A simple, clean, and efficient method for the synthesis of spirooxindole derivatives *via* condensation of isatin with enolizable cyclic β-diketones has been developed. The use of water as a solvent allows avoiding the use of toxic organic solvents, which makes this reaction safe and environmentally friendly. The mechanism of the condensation reaction has been investigated using first-principles-based density functional theory calculations.

INTRODUCTION

The synthesis of spiroheterocycles presents an interesting synthetic challenge to an organic chemist because of their structural rigidity and complexity [1,2]. Spirooxindoles constitute the core structure of many synthetic drugs [3], exhibit remarkable biological properties, and are frequently observed in natural alkaloids [4,5], such as spirotryprostatin B, marefortine, pteropodine, and isopetropodine (Fig. 1). The spiro center provides structural rigidity and complexity to the molecules, thereby increasing its affinity towards proteins by reducing the loss of conformational entropy [6]. Considerable efforts have been directed towards the construction of spirooxindole derivatives in which the classical cyclocondensation method has been used [7]. Consequently, a number of spiro compounds have been obtained with diverse biological activities. These activities mainly include antibacterial, antiviral, anti-inflammatory, and antimicrobial [8]. They are also useful in photodynamic therapy [9].

Xanthene derivatives are also part of many dyes and fluorescent materials for visualization of biomolecules and in laser technologies [10]. Synthetic xanthene derivatives were evaluated as trypanothione reductase inhibitors and chloroquine-potentiating agents [11]. Xanthene derivatives are present as structural building blocks in various natural products exhibiting analgesic, antibacterial [12], antiviral [13], anti-inflammatory [14],

and anti-proliferative [15] activities. The xanthene derivatives are also being utilized as antagonists for paralyzing action of zoxazolamine [16] and in photodynamic therapy [17] and photostable dyes and polymerizable light-emitting dyes [18], in addition to their uses as fluorescent dyes and pH-sensitive fluorescent materials for visualization of biomolecules [19], along with their use in laser technologies [20]. Many xanthene derivatives are also potent nonpeptidic inhibitors of recombinant human calpain I [21] and novel CCRl receptor antagonists [22] (Fig. 2).

Indole moiety is part of various natural products and medicinal agents. In literature, it has been reported that sharing of the indole-3 carbon atom during formation of spiroindoline derivatives greatly enhances its biological activity [23–25]. Mitomycins are natural antibiotics and anticancer compounds acting as DNA cross-linking agents, having an indole moiety [26].

Scanty information is available in the literature concerning the chemistry of such heterocyclic systems containing spirooxindole system and their mass fragmentation studies [27], and no attention seems to have been given to their computational studies. We now wish to report the synthesis and computational studies of new spirooxindole derivatives, that is, 2,3,5,6-tetrahydro-1*H*-spiro[dicyclopenta[*b*,*e*]pyran-8,3′-indoline]1,2′,7-trione and 10*H*,12*H*-spiro[diindeno[1,2-*b*:2′,1′-*e*)pyran-11,3′-indoline]-2′,10,12-trione. Spirooxindole derivatives were also derived in the presence of SBA-15-Pr–SO$_3$H as an
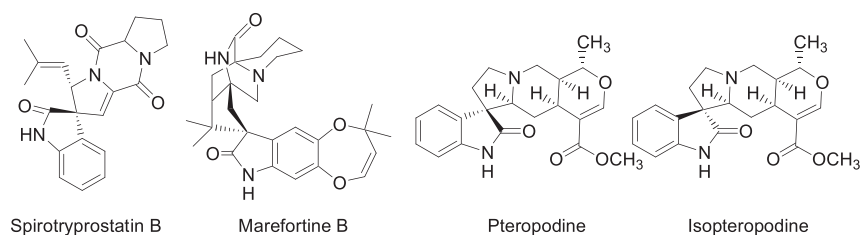
Figure 1. Naturally occurring and biologically active spiroheterocyclic compounds.
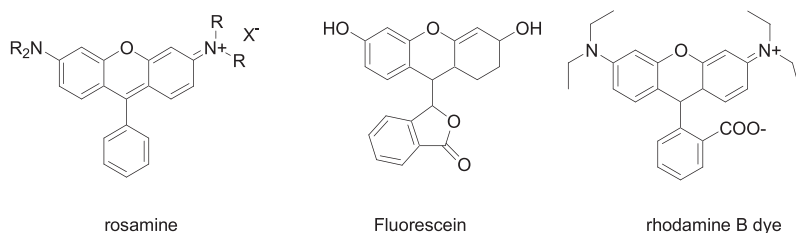
**Figure 2.** Some biologically important xanthene derivatives.

efficient heterogeneous nanosolid acid catalyst [28]. An environmentally benign, readily available, and cost-effective β-cyclodextrin serves as a good alternative to the expensive catalysts containing metals for the synthesis of spirooxindole derivatives [29]. The fluoroboric acid (HBF$_4$) adsorbed on mesoporous silica nanoparticles was probed through a library synthesis of tetraketones or their tautomeric enol forms. These tetraketones are further transformed into xanthenes [30].

As part of our program aimed at developing new selective and environmentally friendly methodologies for the preparation of heterocyclic compounds [31], a number of spirooxindole derivatives have been synthesized through a cyclocondensation reaction employing water as the reaction medium.

RESULTS AND DISCUSSION

The construction of spirooxindole derivatives has been explored by the Knoevenagel condensation of isatin with active methylene group of cyclic β-diketones, which was dehydrated easily to yield the α,β-unsaturated carbonyl compound. The cyclization reaction of appropriate α,β-unsaturated compound with a second molecule of cyclic β-diketone in aqueous medium resulted in the exclusive formation of the spirooxindole products (**11a–h**) in 43–84% yields (Scheme 1). The plausible mechanism of cyclocondensation reaction of isatin derivatives with cyclic β-diketones was shown in Scheme 2. The cyclocondensation reaction of isatin with cyclic β-diketones is carried out with ceric ammonium

Scheme 1. Synthesis of spirooxindole derivatives. [Color figure can be viewed at wileyonlinelibrary.com]
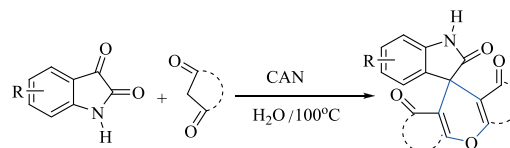
nitrate in water with constant stirring at 100°C. The structure of the new products was unambiguously confirmed by spectral techniques such as IR, ^{1}H-NMR, ^{13}C-NMR, and mass spectroscopies, and the physical data of the synthesized compounds are presented in Table 1.

The >C=O group of isatin in the range of 1720–1750 cm^{-1} disappeared in IR as well as in ^{13}C-NMR in the range of 185–190 ppm, and simultaneously, the appearance of spiro carbon in ^{13}C-NMR in the range of 40–60 ppm was decisively indicative of product formation (**11a–h**). Additional evidence was gathered from the mass spectrum of spirooxindole derivatives. The molecular ion peak and the base peak for **11a** appear at m/z 308 (M + 1) and 276 (100%), respectively. The mass spectrum of spirooxindole product **11b** gave molecular ion peak at m/z 404 (M + 1) and an additional peak at m/z 319 (M–CO), and for compound **11c**, molecular ion peak and other peaks were obtained at 336 (M + 1) and 307 (M–CO) and 214 (M–CO–C$_6$H$_6$O), respectively; **11d** exhibited molecular ion peak and other peaks at 392 (M + 1) and 363 (M–CO) and 307 (M–3CO), respectively.

Scheme 2. Plausible mechanism of cyclocondensation reaction. [Color figure can be viewed at wileyonlinelibrary.com]
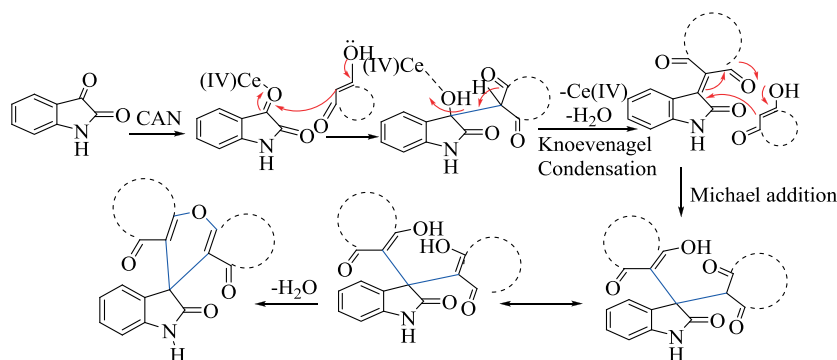
Table 1

Physical data of spirooxindole derivatives (**11a–h**).

Entry	Compound no.	Molecular formula	Time (h)	mp (°C)	Yield (%)
1	**11a**	$C_{18}H_{13}NO_4$	9	>300	43
2	**11b**	$C_{26}H_{13}NO_4$	7	235	78
3	**11c**	$C_{20}H_{17}NO_4$	11	>300	54
4	**11d**	$C_{24}H_{25}NO_4$	4	>300	52
5	**11e**	$C_{18}H_{12}N_2O_6$	3	240	58
6	**11f**	$C_{26}H_{12}N_2O_6$	3	220	84
7	**11g**	$C_{20}H_{16}N_2O_6$	4	110	45
8	**11h**	$C_{24}H_{24}N_2O_6$	4	274	58

A careful literature survey and mechanistic rationale suggest a plausible pathway for the synthesis of spiroheterocycle **11b** as depicted in Scheme 3. Knoevenagel condensation of **1** and **4** would generate isatilidine **8**, which can react with a second molecule of **4** through Michael addition, generating an intermediate **10** followed by water condensation to generate **11b** (Knoevenagel–Michael addition).

EXPERIMENTAL

General procedure.   All chemicals were purchased from Aldrich Chemical Company (St. Louis, MO) and used without further purification. The ^{1}H-NMR and ^{13}C-NMR were obtained from Bruker's 500 spectrometer (at 500 and 125 MHz, respectively) (Bruker, Rheinstetten, Germany), and chemical shifts are reported in ppm scale with respect to CDCl$_3$ 7.269 ppm for ^{1}H-NMR and 77.00 ppm for ^{13}C-NMR as internal standard. Fourier transform infrared spectra were employed on Shimadzu FTIR 8300 spectrophotometer (Kyoto, Japan) for the characterization of the obtained product. Mass spectral studies were performed on XEVO G-2S QTOF. Melting points were determined in open capillary tubes with a Barnstead Electrothermal 9100 BZ circulating oil melting point apparatus and are uncorrected. Analytical thin-layer chromatography was performed using 2.5- to 5-cm plates coated with 0.25 mm thickness of silica gel 60F-254 Merck (Kenilworth, NJ), and visualization was accomplished with ultraviolet light, iodine, and/or KMnO$_4$ staining.

Scheme 3. A plausible mechanism for synthesis of spirooxindole **11b**. [Color figure can be viewed at wileyonlinelibrary.com]
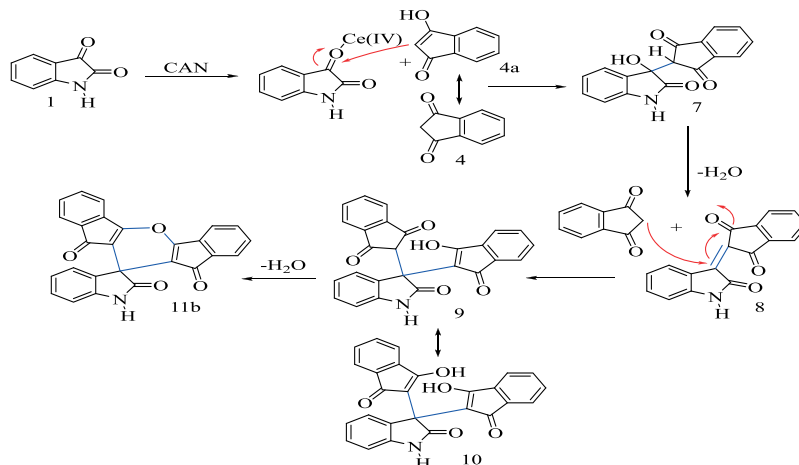
Experimental procedure for the synthesis of spirooxindole derivatives. *General procedure for ceric ammonium nitrate-catalyzed synthesis of spirooxindole derivatives.* A mixture of isatin 1 (1 mmol), β-dicarbonyl compound (2 mmol), and ceric ammonium nitrate (10 mol%) was added to a 50-mL round bottom flask containing water (2 mL) and was stirred at 100°C for an appropriate period of time (4–12 h). After completion of the reaction as indicated by thin-layer chromatography, the reaction mixture was filtered and washed with water to separate the catalyst and then was subjected to column chromatography (with ethyl acetate + petroleum ether) to remove organic impurities. The obtained solution of the desired compound was evaporated, and the residue was recrystallized from ethanol to obtain the pure product.

Characterization of synthesized compounds (11a–h).2,3,5,6-Tetrahydro-1H-spiro[dicyclopenta[b,e]pyran-8,3′-indoline]1,2′,7-trione (11a). $C_{18}H_{13}NO_4$: mp ≥300°C, IR (KBr, cm^{-1}): 3200 (NH), 1740 (>C=O); ^{1}H-NMR (500 MHz, CDCl$_3$) (δ ppm): 2.56 (t, 2CH$_2$), 2.89 (t, 2CH$_2$), 6.90 (dd, 2H), 6.95 (dt, 1H), 7.22 (t, 1H), 7.78 (s,

NH); ^{13}C-NMR (125 MHz, CDCl$_3$) (δ ppm): 14.22, 21.09, 25.40, 29.62, 34.00, 60.43, 110.13, 118.13, 122.79, 123.57, 129.28, 179.35, 199.74 (>C=O); MS (*m/z*): HRMS (ESI) calcd for $C_{18}H_{13}NO_4$ ([M + 1]$^+$): 308.3123; found: 308.2100. *Anal* calcd for $C_{18}H_{13}NO_4$: C, 70.35; H, 4.26; N, 4.56; found: C, 70.30; H, 4.21; N, 4.52.

10H,12H-Spiro[diindeno[1,2-b:2′,1′-e)pyran-11,3′-indoline]-2′,10,12-trione (11b). $C_{26}H_{13}NO_4$: mp 235°C, IR (KBr, cm^{-1}): 3300 (NH), 1735, 1650 (>C=O); ^{1}H-NMR (500 MHz, CDCl$_3$) (δ ppm): 6.77–6.89 (m, Ar–2H), 7.03 (d, Ar–2H), 7.15–7.19 (m, Ar–4H), 7.99–8.03 (m, Ar–4H), 8.33 (NH); ^{13}C-NMR (125 MHz, CDCl$_3$) (δ ppm): 52.38, 60.43, 110.33, 122.82, 123.21, 123.31, 123.35, 123.76, 128.03, 129.32, 135.65, 135.91, 137.30, 141.50, 142.38, 171.22, 175.94; MS (*m/z*): HRMS (ESI) calcd for $C_{26}H_{13}NO_4$ ([M + 1]$^+$): 404.0918; found: 404.2084. *Anal* calcd for $C_{26}H_{13}NO_4$: C, 77.41; H, 3.25; N, 3.44; found: C, 77.42; H, 4.18; N, 4.50.

3′,4′,6′,7′-Tetrahydrospiro[indoline-3,9′-xanthene]-1′,2,8′(2′H,5′H)-trione (11c). $C_{20}H_{17}NO_4$: mp ≥300°C, IR (KBr, cm^{-1}): 3350 (NH), 1740, 1650 (>C=O); ^{1}H-NMR
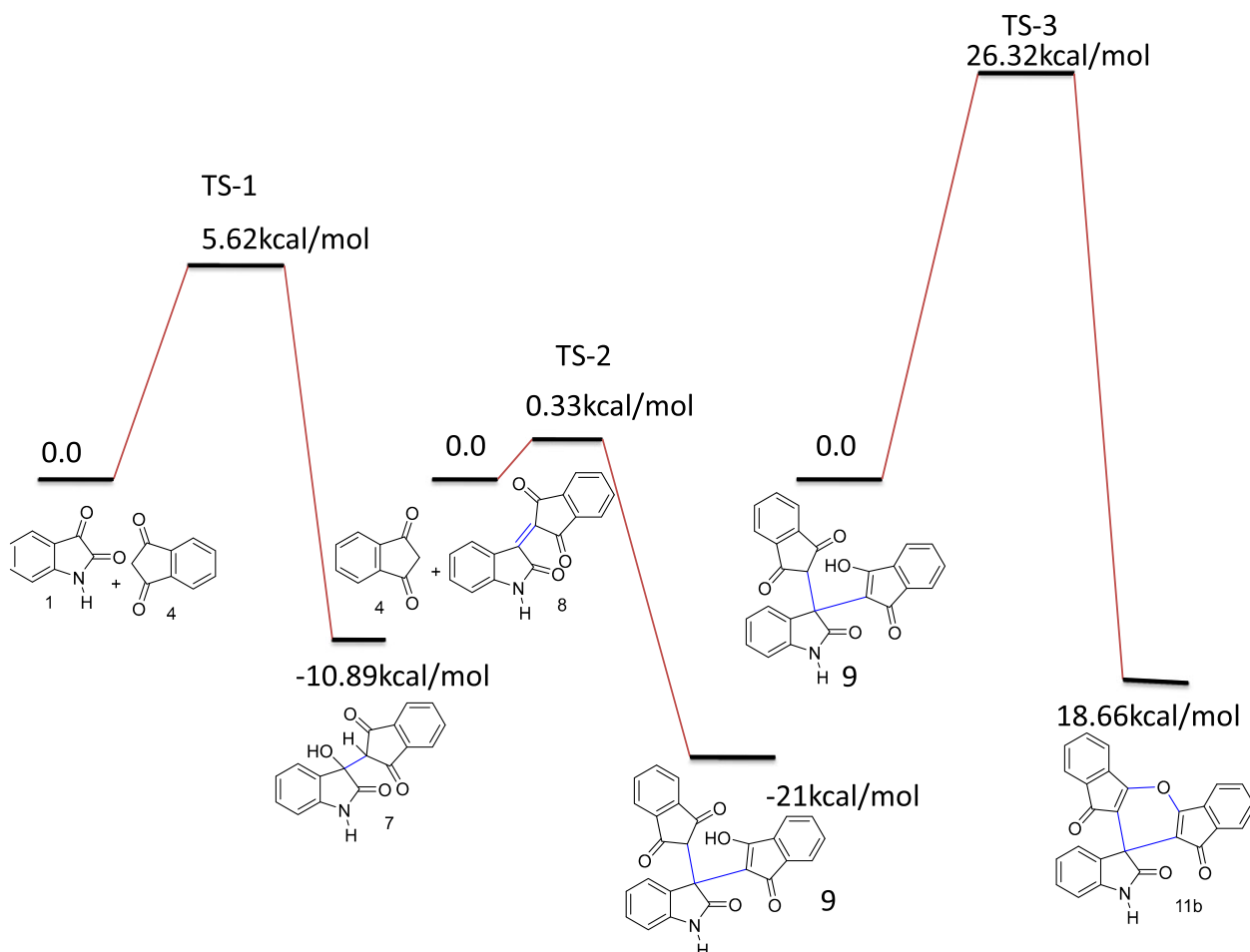
Figure 3. Energy profile diagram for synthesis of **11b**. [Color figure can be viewed at wileyonlinelibrary.com]

(500 MHz, CDCl$_3$) (δ ppm): 1.93–1.99 (m, 4H, 2CH$_2$), 2.03–2.10 (m, 4H, 2CH$_2$), 2.64 (t, 4H, 2CH$_2$), 6.85–7.25 (m, Ar–H), 7.60 (s, NH); ^{13}C-NMR (125 MHz, CDCl$_3$) (δ ppm): 20.01, 27.58, 41.1, 45.89 (spiro-C), 109.20, 114.82, 121.91, 122.69, 128.47, 133.80, 142.34, 164.9, 179.08 (>C=O), 195.39 (>C=O); MS (*m/z*): HRMS (ESI) calcd for C$_{20}$H$_{17}$NO$_4$ ([M + 1]$^+$): 336.1231; found: 336.2078. *Anal* calcd for C$_{20}$H$_{17}$NO$_4$: C, 71.63; H, 5.11; N, 4.18; found: C, 71.60; H, 5.09; N, 4.16.

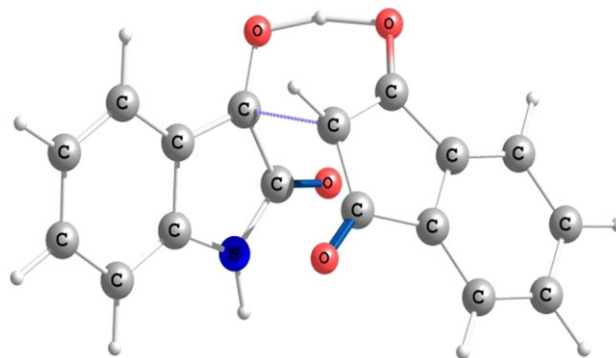*3′,3′,6′,6′-Tetramethyl-3′,4′,6′,7′-tetrahydrospiro[indoline-3,9′-xanthene]-1′,2,8′(2′H,5′H)-trione (11d).* C$_{24}$H$_{25}$NO$_4$: mp ≥300°C, IR (KBr, cm^{-1}): 3200 (NH), 1650 (>C=O); ^{1}H-NMR (500 MHz, CDCl$_3$) (δ ppm): 1.03 (s, 6H, 2CH$_3$), 1.11 (s, 6H, 2CH$_3$), 2.14 (s, 4H, CH$_2$), 2.53 (s, 2H, CH$_2$), 2.54 (s, 2H, CH$_2$), 6.85–6.88 (m, Ar–3H), 7.14 (t, Ar–1H), 8.06 (s, NH); ^{13}C-NMR (125 MHz, CDCl$_3$) (δ ppm): 27.17, 28.98, 31.98, 41.27, 50.95 (spiro-C), 109.58, 113.55, 122.00, 122.29, 128.51, 133.65, 142.33, 163.62, 178.92 (>C=O), 195.38 (>C=O); MS (*m/z*): HRMS (ESI) calcd for C$_{24}$H$_{25}$NO$_4$ ([M + 1]$^+$): 392.1857; found: 392.2856. *Anal* calcd for C$_{24}$H$_{25}$NO$_4$: C, 73.64; H, 6.44; N, 3.58; found: C, 73.60; H, 6.49; N, 4.60.

5′-Nitro-2,3,5,6-tetrahydro-1H-spiro[dicyclopenta[b,e]pyran-8,3′-indoline]-1,2′,7-trione (11e). C$_{18}$H$_{12}$N$_2$O$_6$: mp 240°C; IR (KBr, cm^{-1}): 3350, 1745, 1650; ^{1}H-NMR (500 MHz, CDCl$_3$) (δ ppm): 2.49 (t, 4H, 2CH$_2$), 3.79 (t, 4H, 2CH$_2$), 6.66–7.80 (m, Ar–H), 10.81 (s, NH); ^{13}C-NMR (125 MHz, CDCl$_3$) (δ ppm): 29.18, 35.50, 46.13 (spiro-C), 105.29, 112.80, 114.82, 121.67, 125.12, 144.21, 148.31, 160.1, 175.26 (>C=O), 195.07 (>C=O); MS (*m/z*): HRMS (ESI) calcd for C$_{18}$H$_{12}$N$_2$O$_6$ ([M + 1]$^+$): 353.0768; found: 353.1028. *Anal* calcd for C$_{18}$H$_{12}$N$_2$O$_6$: C, 61.37; H, 3.43; N, 7.95; found: C, 61.39; H, 3.45; N, 7.97.

5′-Nitro-10H,12H-spiro[diindeno[1,2-b:2′,1′-e)pyran-11,3′-indoline]-2′,10,12-trione (11f). C$_{26}$H$_{12}$N$_2$O$_6$: mp 220°C; IR (KBr, cm^{-1}): 3400, 1745, 1660; ^{1}H-NMR (500 MHz, CDCl$_3$) (δ ppm): 6.98–8.15 (m, Ar–H), 10.65 (s, NH); ^{13}C-NMR (125 MHz, CDCl$_3$) (δ ppm): 45.91 (spiro-C), 126.7, 128.3, 128.7, 129.45, 134.2, 134.4, 136.1, 144.5, 148.2, 160.0, 168.2 (>C=O), 187.0 (>C=O); MS (*m/z*): HRMS (ESI) calcd for C$_{26}$H$_{12}$N$_2$O$_6$ ([M + 1]$^+$): 448.0695; found: 448.1995. *Anal* calcd for C$_{26}$H$_{12}$N$_2$O$_6$: C, 69.65; H, 2.70; N, 6.25; found: C, 69.67; H, 2.72; N, 6.23.

5-Nitro-3′,4′,6′,7′-tetrahydrospiro[indoline-3,9′-xanthene]1′,2,8′(2′H,5′H)-trione (11g). C$_{20}$H$_{16}$N$_2$O$_6$: mp 110°C; IR (KBr, cm^{-1}): 3460, 1722, 1665; ^{1}H-NMR (500 MHz, DMSO-d_6) (δ ppm): 1.03 (t, 4H, 2CH$_2$), 1.27–1.32 (t, 4H, 2CH$_2$), 1.38 (t, 4H, 2CH$_2$), 5.89 (t, Ar–1H), 5.99 (d, Ar–1H), 6.19 (t, Ar–1H), 9.44 (s, NH); ^{13}C-NMR (125 MHz, DMSO-d_6) (δ ppm): 20.20, 27.37, 37.46, 45.81 (spiro-C), 108.71, 121.09, 123.12, 128.1, 134.75, 144.26, 148.31, 165.57, 178.85 (>C=O), 195.62

(>C=O); MS (*m/z*): HRMS (ESI) calcd for C$_{20}$H$_{16}$N$_2$O$_6$ ([M + 1]$^+$): 381.1081; found: 381.2126. *Anal* calcd for C$_{20}$H$_{16}$N$_2$O$_6$: C, 63.16; H, 4.24; N, 7.37; found: C, 63.19; H, 4.25; N, 7.39.

Figure 4. Optimized molecular structure of TS-1. [Color figure can be viewed at wileyonlinelibrary.com]
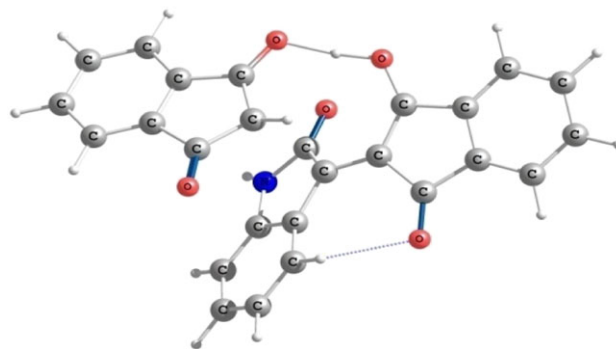
Figure 5. Optimized molecular structure of TS-2. [Color figure can be viewed at wileyonlinelibrary.com]
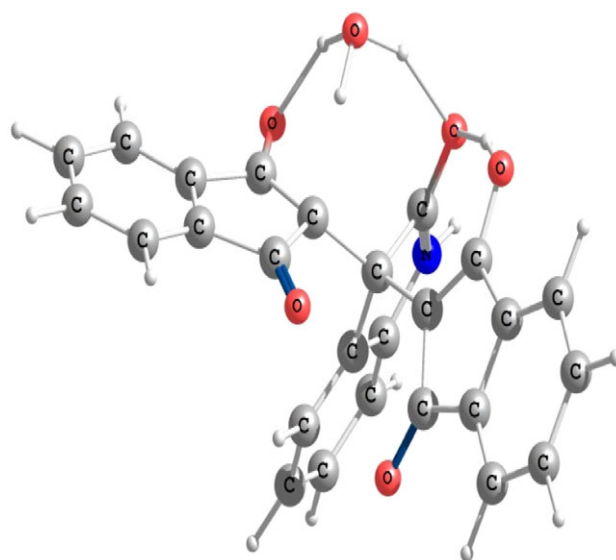
Figure 6. Optimized molecular structure of TS-3. [Color figure can be viewed at wileyonlinelibrary.com]

*5-Nitro-3′,3′,6′,6′-tetramethyl-5-nitro-3′,4′,6′,7′-tetrahydrospiro[indoline-3,9′-xanthene]-1′,2,8′(2′H,5′H)-trione (11h).* $C_{24}H_{24}N_2O_6$: mp 274°C; IR (KBr, cm^{-1}): 3360, 1720, 1665; ^{1}H-NMR (500 MHz, CDCl$_3$) (δ ppm): 1.09 (s, 6H, 2CH$_3$), 1.17 (s, 6H, 2CH$_3$), 2.21 (4H, s, CH$_2$), 2.32 (4H, s, CH$_2$), 6.96–8.33 (4H, m, Ar–H), 8.53 (s, NH); ^{13}C-NMR (125 MHz, CDCl$_3$) (δ ppm): 27.10, 29.01, 33.07, 43.25, 46.49, 54.60 (spiro-C), 109.81, 110.94, 116.62, 125.78, 133.73, 143.46, 149.05, 170.39, 181.79 (>C=O), 195.82 (>C=O); MS (*m/z*): HRMS (ESI) calcd for $C_{24}H_{24}N_2O_6$ ([M + 1]$^+$): 436.1634; found: 436.2011. *Anal* calcd for $C_{24}H_{24}N_2O_6$: C, 66.05; H, 5.54; N, 6.42; found: C, 66.07; H, 5.56; N, 6.43.
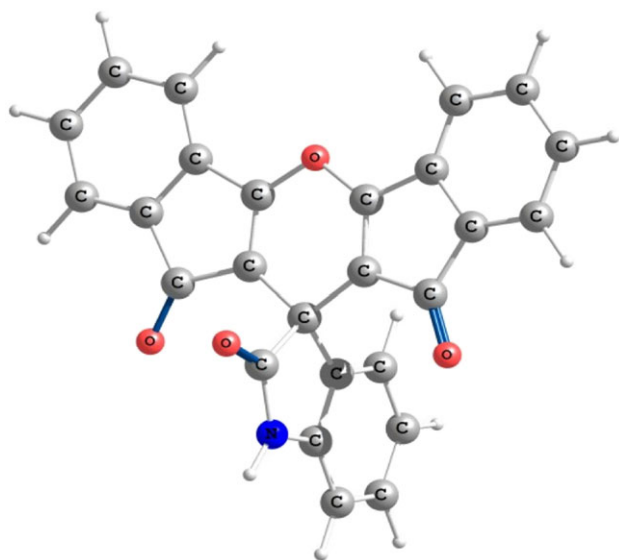

Figure 7. Optimized molecular structure of product **11b**. [Color figure can be viewed at wileyonlinelibrary.com]

COMPUTATIONAL DETAILS

To validate the proposed reaction mechanism, we carried out first-principles-based theoretical calculations using the density functional theory-based triple hybrid B3LYP functional [32]. The initial conformational search for each reactants, intermediates, and products was performed at B3LYP/6-31G* level of theory. Considering the lowest energy structures for each case, further full geometry optimization and subsequent harmonic frequency calculations were performed using B3LYP with 6-31G** basis [33], to determine the extrema for all the reactants, intermediates, and products. The corresponding transition states were explored by looking at the reaction and product intermediates. Each minima were confirmed by no imaginary frequency, and transition states at each step were confirmed by a single imaginary frequency characterized by the corresponding desired reaction coordinates. The vibrational zero-point energy was considered for all the molecules in evaluating the final energy profiles of the suggested reaction mechanisms as (Fig. 3) shown in Scheme 3. All the calculations were carried out with Gaussian 09 program suit [34].

We started with the reaction of **1** with the enol form of **4**. In the first step, enolic carbon attacked the carbonyl carbon with a concerted proton transfer from enolic oxygen to carbonyl oxygen forming a six-membered transition state. The optimized structure of this first transition state was shown in Figure 4. The corresponding reaction barriers are found to be only 5.62 kcal/mol, which shows the high feasibility of this step. This reaction is exothermic by 10.89 kcal/mol, which shows that this step is kinetically as well as thermodynamically favorable. This is followed by water elimination, which formed an α,β-unsaturated compound

(11a)   (11b)   (11c)   (11d)

(11e)   (11f)   (11g)   (11h)
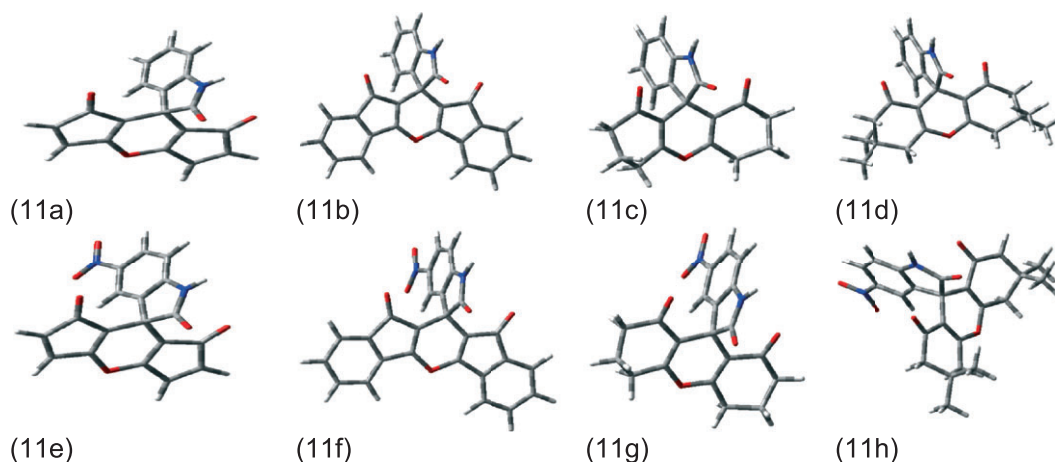
Figure 8. Optimized geometries of spirooxindole derivatives. [Color figure can be viewed at wileyonlinelibrary.com]
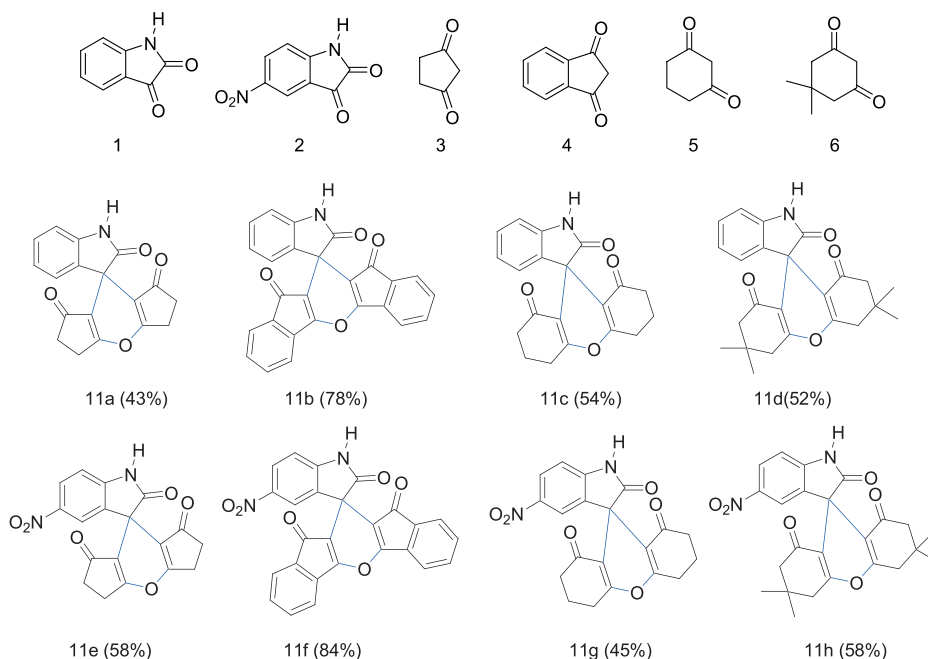
Figure 9. Reactants and products. [Color figure can be viewed at wileyonlinelibrary.com]

8. In the next step, another cyclic 1,3-dione (**4**) attacked to carbon of α,β-unsaturated compound with a proton transfer to oxygen *via* six-membered transition state. The optimized structure of this second transition state was shown in Figure 5. We found the barrier of this step is very low (0.33 kcal/mol), which indicates that this step is instantaneous and the reaction is once again exothermic by ~21 kcal/mol with a formation of the product **9**. The next step is the keto–enol tautomerization to form **9** (keto form) to **10** (enol form). It was happened through transition state **3** and the optimized structure of third transition state shown in Figure 6. The reaction barrier for the tautomerization is found to be 26.32 kcal/mol, which was followed by water elimination to form the product **11b**. Optimized structure of the product **11b** was shown in Figure 7. Overall, it is found that the proposed mechanism is highly favorable for the formation of **11b** starting from **1** and **4**. Optimized geometries of all spirooxindole derivatives from **11a** to **11h** were shown in Figure 8. All the optimized geometries were carried out with Gaussian 09 program suit. Structure of all types of reactants and synthesized spirooxindole derivatives from **11a** to **11h** was shown in Figure 9.

CONCLUSIONS

An expedient, delicate, and efficient cyclocondensation methodology giving higher yields for the facile synthesis

of spirooxindole derivatives has been reported. A significant observation of the reported method is the employment of greener approach using water as a solvent and environmentally benign protocol. This cyclocondensation process involves formation of two C–C bonds and two C–O bonds during synthesis of the spirooxindoles. This protocol would have significant relevance in the area of pharmaceutical and medicinal chemistry.

Significance of the work.   Ceric ammonium nitrate (CAN) can be easily soluble in water and easily removed from crude product by washing from water and easily recrystallized from ethanol. CAN provides good oxidizing ability to synthesize spirooxindoles rather than other catalyst.

In terms of CAN, redox process Ce(IV) is converted to Ce(III), one negative electron change signaled by the fading of the solution color from orange to pale yellow; thus, it also works as indicator to complete the reaction.

Products **11a**, **11b**, **11e**, and **11f** have been constructed with appropriate yield. These compounds have not been reported in any journal. We are delivering here a new methodology or experimental criteria for the synthesis of these compounds.

Furthermore, the computational criterion is one of the most important terms in providing the better reaction pathway (mechanism) to understanding the transition state (TS) and stability of the product by optimizing the energy profile diagram.

REFERENCES AND NOTES

[1] Begum, T.; Molvi, K. I.; Khan, S. A. World J. Pharm. Pharm. Sci. 2014, 3, 42.

[2] (a) Padamavati, V.; Sudheer, K.; Muralikrishna, A.; Padmaja, A. Indian J. Chem. 2015, 54B, 283; (b) Jiang, B.; Cao, L. J.; Tu, S. J.; Zheng, W. R.; Yu, H. Z. J. Comb. Chem. 2009, 11, 612.

[3] Chen, H.; Shi, D. J. Comb. Chem. 2010, 12, 571.

[4] Dandia, A.; Singh, R.; Khaturia, S.; Merienne, C.; Morgant, G.; Loupy, A. Bioorg Med Chem 2006, 14, 2409.

[5] Tan, B.; Hernandez-Torres, G.; Barbas, C. J. Am. Chem. Soc. 2011, 133, 12354.

[6] Campoy, A. V.; Todd, M. J.; Freire, E. Biochemistry 2000, 39, 2201.

[7] Dandia, A.; Parewa, V.; Jain, A. K.; Rathore, K. S. Green Chem. 2011, 13, 2135.

[8] Bhaskar, G.; Yuvaraj, A.; Chandrasekar, B.; Chandrasekara, S.; PerumalParamasivan, T. Eur. J. Med. Chem. 2012, 51, 79.

[9] Knight, C. G.; Stephenes, T. Biochem. J. 1989, 258, 683.

[10] Sirkercioglu, O.; Tulinli, N.; Akar, A. J Chem Res 1995, 12, 502.

[11] Chibale, K.; Visser, M.; Van Schalkwyk, D.; Smith, P. J.; Saravanamuthu, A.; Fairlamb, A. H. Tetrahedron 2003, 59, 2289.

[12] (a) Wang, H.; Lu, L.; Zhu, S.; Li, Y.; Cai, W. Curr. Microbiol. 2006, 52, 1; (b) Limsuwan, S.; Trip, E. N.; Kouwen, T. R. H. M.; Piersma, S.; Hiranrat, A.; Mahabusarakam, W.; Voravuthikunchai, S. P.; Kayser, J. M. V. D. Phytomedicine 2009, 16, 645.

[13] Jamison, J. M.; Krabill, K.; Hatwalker, A.; Jamison, E.; Tsai, C. Cell Biol. Int. Rep. 1990, 14, 1075.

[14] (a) Kefayati, H.; Bazargard, S. J.; Vejdansefat, P.; Shariati, S.; Kohankar, A. M. Dyes and pigments 2016, 125, 309; (b) Hafez, H. N.; Hegab, M. I.; Ahmed-Farag, I. S.; ElGazzar, A. B. A. Bioorg. Med. Chem. Lett. 2008, 18, 4538.

[15] Kumar, A.; Sharma, S.; Maurya, R. A.; Sarkar, J. J. Comb. Chem. 2010, 12, 20.

[16] Saint-Ruf, G.; De, A.; Hieu, H. T. Bull ChimTher 1972, 7, 83.

[17] Ion, R. M.; Planner, A.; Wiktorowicz, K.; Frackowiak, D. Acta Biochim. Pol. 1998, 45, 833.

[18] (a) Bojinov, V. B.; Panova, I. P.; Simeonov, D. B. Dyes Pigm 2009, 83, 135; (b) Bojinov, V. B.; Panova, I. P.; Grabchev, I. K. Dyes Pigm 2007, 74, 187.

[19] (b) Prasad, D.; Preetam, A.; Nath, M. C. R. Chimie 2012, 15, 675.

[20] Kumar, R.; Nandi, G. C.; Verma, R. C.; Singh, M. S. Tetrahedron Lett. 2010, 51, 442.

[21] Chatterjee, S.; Iqbal, M.; Kauer, J. C.; Mallamo, J. P.; Senadhi, S.; Mallya, S.; Bozyczko-Coyne, D.; Siman, R. Bioorg. Med. Chem. Lett. 1996, 6, 1619.

[22] Naya, A.; Ishikawa, M.; Matsuda, K.; Ohwaki, K.; Saeki, T.; Noguchi, K.; Ohtake, N. Bioorg. & Med. Chern 2003, 11, 875.

[23] Da-Siva, J. F. M.; Garden, S. J.; Pinto, A. C. J. Braz. Chem. Soc. 2001, 12, 273.

[24] Abdel-Rahman, A. H.; Keshk, E. M.; Hanna, M. A.; El-Bady, S. M. Bioorg Med Chem 2483, 2004, 12.

[25] Zhu, S. L.; Ji, S. J.; Jong, Z. Tetrahedron 2007, 63, 9365.

[26] Miller, K. A.; Tsukamoto, S.; Williams, R. M. Nat. Chem. 2009, 1, 63.

[27] Joshi, K. C.; Jain, R.; Aroma, S. Journal of Fluorine Chemistry 1989, 42, 149.

[28] Ziarani, G. M.; Lashgari, N.; Badiei, A. R. Scientia Iranica, C 2013, 20, 580.

[29] Srivastava, M.; Rai, P.; Yadav, S.; Tripathi, B. P.; Mishra, A.; Singh, J.; Singh, J. J. Indian Chem. Soc. 2016, 93, 843.

[30] Ray, S.; Bhaumik, A.; Pramanik, M.; Butcher, R. J.; Yildirim, S. O.; Mukhopadhyay, C. Cat. Com. 2014, 43, 173.

[31] (a) Sharma, S.; Pathare, R. S.; Maurya, A. K.; Gopal, K.; Roy, T. K.; Sawant, D. M.; Pardasani, R. T. Org. Lett. 2016, 18, 356; (b) Maloo, P.; Roy, T. K.; Sawant, D. M.; Pardasani, R. T.; Salunkhe, M. M. RSC Adv. 2016, 6, 41897; (c) Pathare, R. S.; Sharma, S.; Elagandhula, S.; Saini, V.; Sawant, D. M.; Yadav, M.; Sharon, A.; Khan, S.; Pardasani, R. T. Eur. J. Org. Chem. 2016, 33, 5579; (d) Pathare, R. S.; Sharma, S.; Kandasamy, G.; Sawant, D. M.; Pardasani, R. T. Tetrahedron Lett. 2017, 58, 1387; (e) Sawant, D. M.; Singh, I.; Tulsyan, G.; Abbagani, K.; Pardasani, R. T. Synlett 2015, 26, 1671.

[32] (a) Becke, A. D. Phys. Rev. A 1988, 38, 309; (b) Lee, C.; Yang, W.; Parr, R. G. Phys Rev B 1988, 37, 785.

[33] (a) Clark, T.; Chandrasekhar, J.; Spitznagel, G. W.; Schleyer, P. V. R. J. Comput. Chem. 1983, 4, 294; (b) Frisch, M. J.; John, A. P.; Stephen Binkley, J. J ChemPhys 1984, 80, 3265.

[34] Frisch, M. J.; Trucks, G. W.; Schlegel, H. B.; Scuseria, G. E.; Robb, M. A.; Cheeseman, J. R.; Scalmani, G.; Barone, V.; Petersson, G. A.; Nakatsuji, H.; Li, X.; Caricato, M.; Marenich, A.; Bloino, J.; Janesko, B. G.; Gomperts, R.; Mennucci, B.; Hratchian, H. P.; Ortiz, J. V.; Izmaylov, A. F.; Sonnenberg, J. L.; Williams-Young, D.; Ding, F.; Lipparini, F.; Egidi, F.; Goings, J.; Peng, B.; Petrone, A.; Henderson, T.; Ranasinghe, D.; Zakrzewski, V. G.; Gao, J.; Rega, N.; Zheng, G.; Liang, W.; Hada, M.; Ehara, M.; Toyota, K.; Fukuda, R.; Hasegawa, J.; Ishida, M.; Nakajima, T.; Honda, Y.; Kitao, O.; Nakai, H.; Vreven, T.; Throssell, K.; Montgomery, J. A.; Peralta, J. E.; Ogliaro, F.; Bearpark, M.; Heyd, J. J.; Brothers, E.; Kudin, K. N.; Staroverov, V. N.; Keith, T.; Kobayashi, R.; Normand, J.; Raghavachari, K.; Rendell, A.; Burant, J. C.; Iyengar, S. S.; Tomasi, J.; Cossi, M.; Millam, J. M.; Klene, M.; Adamo, C.; Cammi, R.; Ochterski, J. W.; Martin, R. L.; Morokuma, K.; Farkas, O.; Foresman, J. B.; Fox, D. J. Gaussian 09, revision D; Inc.Wallingford CT: Gaussian, 2010; Vol 01.